ISSN (Print) 1226-1750
ISSN (Online) 2233-6656
Journal of Magnetics 25(1), 43-47 (2020) https://doi.org/10.4283/JMAG.2020.25.1.043

Effect of Nd Substitution for Mischmetal on Magnetic Properties in (MM,Nd)-Fe-B Ribbons

Zhu-bai Li[1]*, Jing-zhao Li[1,2], Zhi-yi Xu[3], Yong-feng Li[1,2], and Xue-feng Zhang[1,2]

[1]*Key Laboratory of Integrated Exploitation of Bayan Obo Multi-Metal Resources, Inner Mongolia University of Science and Technology, Baotou 014010, China*
[2]*School of science, Inner Mongolia University of Science and Technology, Baotou 014010, China*
[3]*National Institute of Metrology, Beijing 100029, China*

(Received 16 February 2018, Received in final form 22 February 2020, Accepted 24 February 2020)

Mischmetal-based permanent magnets of $(MM,Nd)_{12}Fe_{82}B_6$ were prepared by melt-spinning method via varying the relative content of mischmetal and Nd. The coercivity is low, and the squareness of hysteresis loop is poor in $MM_{12}Fe_{82}B_6$ ribbons. The x-ray diffraction pattern, maximum of δm value as well as the temperature dependence of magnetization indicates that the partial substitution of Nd for MM could improve the crystallinity in the mischmetal-based magnets, and both the coercivity and squareness of hysteresis loop increase with Nd substitution for mischmetal. The increase of squareness should be partially attributed to the improvement in the crystallinity of $R_2Fe_{14}B$ crystal phase. For more than 4 at.% Nd substitution the coercivity is not less than that in corresponding (Ce,Nd)-based magnets, and the coercivity of 7.81 kOe and the maximum energy product of 15.41 MGOe were obtained in $MM_8Nd_4Fe_{82}B_6$ ribbons. These investigations show that it is reasonable to use the low cost mischmetal to prepare the resource-saving rare-earth magnets, and that optimizing the addition amount of Nd is necessary to improve the crystallinity and enhance the magnetic properties.

Keywords : permanent magnets, mischmetal, crystallinity, coercivity

1. Introduction

Abundant rare-earth elements La and Ce are expected to substitute for Nd in $Nd_2Fe_{14}B$ permanent magnets in order to utilize efficiently the rare-earth elements as well as to reduce the production cost [1-8]. However, the coercivity is rather low in ternary alloys of Ce-Fe-B and La-Fe-B [9-11], and the addition of Nd element is necessary in (La,Ce)-Fe-B alloys to improve the coercivity [10-12]. La, Ce, Pr and Nd elements coexist in rare-earth resource, which is referred as mischmetal, and purifying the simple substance is more costly than purifying the mischmetal. It seems more reasonable to prepare the resource-saving rare-earth magnets using mischmetal rather than using the mixture of simple substances Ce and Nd [13-15]. The magnetic properties of $(La\text{-}Ce)_2Fe_{14}B$ are different from those of $(Pr\text{-}Nd)_2Fe_{14}B$ [16-19]. Is the effect of mischmetal better than that of the mixing of Ce and Nd elements in preparing the resource-saving rare-earth magnets? In this paper, (MM,Nd)-Fe-B (MM denotes mischmetal) magnets were prepared using mischmetal, and the magnetic properties were investigated by varying the substitution amount of Nd element, which are expected to serve as a reference for the preparation of the resource-saving rare-earth magnets using the low cost mischmetal.

2. Experimental

The commercial mischmetal, Nd, Fe and Fe-B alloy were mixed according to the nominal composition of $MM_{12-x}Nd_xFe_{82}B_6$ (x = 0, 1, 2, 4, 7, 10, and 12). The purity of mischmetal is more than 99 wt.%, and the content of rare-earth elements is similar to that in minerals, i.e., La/R~28.27 wt.%, Ce/R~50.46 wt.%, Pr/R~5.22 wt.%, Nd/R~15.66 wt.%, Sm/R~less than 0.05 wt.% and other inevitable impurities. The mixture was melted by arc-melting under an argon atmosphere, and the obtained ingot was turned over and re-melted three times to ensure compositional homogeneity. About 2.5 g of ingot was re-

*Corresponding author: Tel: +86-472-5953508
Fax: +86-472-5953508, e-mail: lzbgj@163.com

melted by induction melting and then ejected onto the surface of a rotating copper wheel by pressurized argon. The surface velocity of copper wheel was varied in the range of 25-27 m/sec for optimizing both the coercivity and the squareness of hysteresis loop. X-ray diffraction (XRD) using Co Kα radiation was employed to check the microstructure. The hysteresis loops and magnetization dependence on temperature were measured using Lakeshore vibrating sample magnetometer (VSM), and the plane of the ribbon is in the field direction and therefore the demagnetization factor was neglected.

3. Results and Discussion

The hysteresis loops are shown in Fig. 1 for these $(MM,Nd)_{12}Fe_{82}B_6$ ribbons. On the initial magnetization curve the magnetization increases slowly with increasing the applied field under the low field, implying that the pinning effect of domain wall motion is dominant in the magnetization process due to the nanostructure in the ribbons. Both the coercivity and maximum energy product increase monotonically with the increase of Nd content. The squareness of hysteresis loop, obtained by the ratio of $\int_0^{-H_c} M/M_s dH$ in the second quadrant to $M_r/M_s * H_c$ (the product of reduced remanence and coercivity), is shown in the inset of Fig. 1. The squareness increases for the substitution of Nd for mischmetal. Fig. 2 shows the coercivity and the maximum energy product of $(MM,Nd)_{12}Fe_{82}B_6$ ribbons, and the coercivity of $(Ce,Nd)_{12}Fe_{82}B_6$ ribbons is also shown in Fig. 2 [10]. The anisotropy field of $La_2Fe_{14}B$, 20 kOe, isn't much different from 26 kOe of $Ce_2Fe_{14}B$. For $Pr_2Fe_{14}B$ and $Nd_2Fe_{14}B$ the magnetocrystalline anisotropy fields are 75 kOe and 73 kOe, respectively, which are nearly the same [16]. So the coercivity could be compared between $(MM,Nd)_{12}Fe_{82}B_6$ and $(Ce,Nd)_{12}Fe_{82}B_6$ according to the relative content of La-Ce and Pr-Nd, since the content of other rare-earth elements is much lower and could be neglected in this mischmetal. In $MM_{10}Nd_2Fe_{82}B_6$ the content of La-Ce is nearly the same with that in $Ce_8Nd_4Fe_{82}B_6$, but the coercivity of 5.95 kOe is lower than 6.84 kOe of $Ce_8Nd_4Fe_{82}B_6$. While in $MM_5Nd_7Fe_{82}B_6$ ribbons La-Ce content is nearly the same with Ce content in $Ce_4Nd_8Fe_{82}B_6$, and the coercivities are nearly the same. In $MM_2Nd_{10}Fe_{82}B_6$ ribbons the coercivity is more than that of corresponding $(Ce,Nd)_{12}Fe_{82}B_6$ ribbons. These facts suggest that the effect of mischmetal on the magnetic properties is different from that for the mixture of Ce and Nd elements. It is more reasonable to prepare the resource-saving magnets using the less costly rare-earth of mischmetal. The coercivity of 7.81 kOe and the maximum energy product of 15.41 MGOe were obtained.

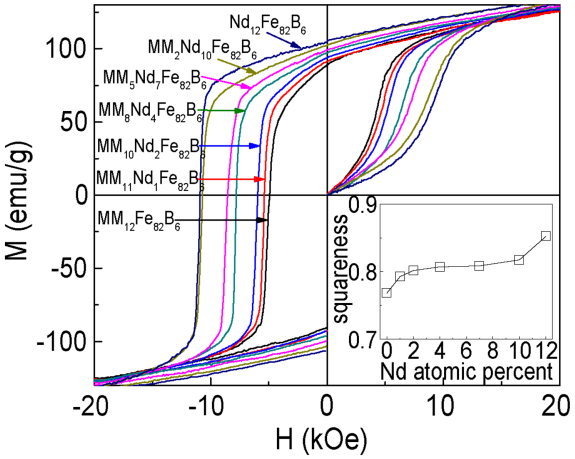

Fig. 1. (Color online) The hysteresis loops for (MM,Nd)-Fe-B ribbons at room temperature, and the inset shows the dependence of squareness on the MM atomic percent.

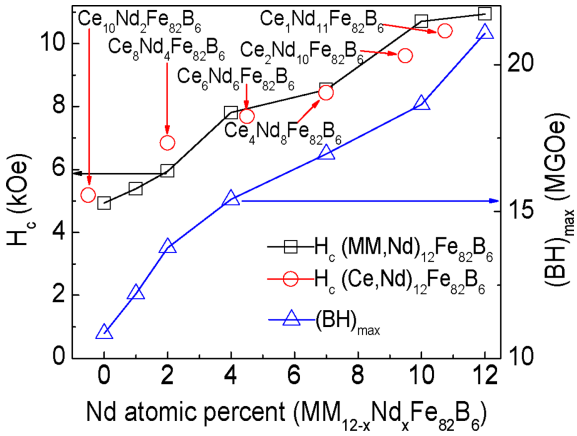

Fig. 2. (Color online) The dependences of coercivity and maximum energy product on the atomic percent of mischmetal in $MM_{12-x}Nd_xFe_{82}B_6$ ribbons.

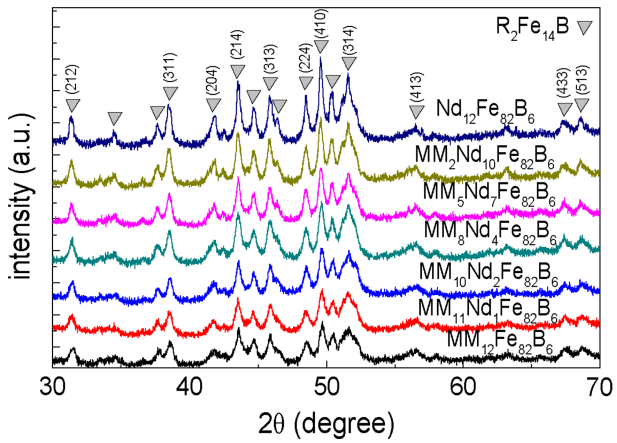

Fig. 3. (Color online) XRD patterns obtained by using Co Kα radiation for (MM,Nd)-Fe-B ribbons.

ed in $MM_8Nd_4Fe_{82}B_6$ ribbons.

In permanent magnets the coercivity is sensitive to the microstructure. Fig. 3 shows the XRD patterns of these ribbons, on which the diffraction peaks correspond to $R_2Fe_{14}B$ crystal phase. According to the half height width of the diffraction peaks the grain sizes are estimated to be in the range of 20-30 nm using JADE software. The intensities of diffraction peaks are weaker in $MM_{12}Fe_{82}B_6$, $MM_{11}Nd_1Fe_{82}B_6$ and $MM_{10}Nd_2Fe_{82}B_6$ ribbons, indicating the low crystallinity of $R_2Fe_{14}B$ phase. There should coexist the amorphous phase and the minor crystalline phase, such as RFe_2 in these ribbons [20]. The measuring sensitivity is low for this x-ray diffractometer using Co Kα radiation, though the measurement noise is weak. The low crystallinity and the large amount of amorphous phase could deteriorate the magnetic properties. For Nd substitution for mischmetal the intensities of diffraction peaks become stronger, suggesting an increase in the crystallinity of $R_2Fe_{14}B$ phase. The structure of $La_2Fe_{14}B$ crystal is less stable than that of $Nd_2Fe_{14}B$ crystal [21], so the variation of crystallinity may be related to the difference in the structure stability of $R_2Fe_{14}B$ crystal for La, Ce, Pr and Nd.

$R_2Fe_{14}B$ is tetragonal structure, and the lattice constant could be obtained via the cell refinement using Jade software. Table 1 lists $R_2Fe_{14}B$ lattice constant and magnetic properties for these ribbons. In $MM_{12}Fe_{82}B_6$ ribbons the lattice constants a and c are 8.79 Å and 12.22 Å, respectively, larger than 8.76 Å and 12.11 Å of $Ce_2Fe_{14}B$, but less than 8.82 Å and 12.34 Å of $La_2Fe_{14}B$ [16]. Different with other rare-earth ions, Ce ion has an assessed 3.44 mixed valence of tetravalent $4f^0$ and trivalent $4f^1$ electronic states, and its ionic radius is the lowest in the rare-earth [22]. Nd bears larger ionic size than Ce [22], and so a little amount substitution of Nd element leads to an increases of lattice constants a and c. The shift of Ce valence between the quadrivalence to trivalence could also lead to an increase of lattice constants [22, 23]. However, for a larger amount of Nd substitution the lattice constant c decreases in $MM_5Nd_7Fe_{82}B_6$ and $MM_2Nd_{10}Fe_{82}B_6$. Both the decrease of La content and the improvement of crystallity can give rise to the decrease of lattice constants. The sizes of rare-earth ions are different in mischmetal [16], and the structure of MM-based magnets is more complicated than that of the simple substance rare-earth-based magnets of $Nd_2Fe_{14}B$.

Table 1. Lattice parameters and magnetic properties for (MM,Nd)-Fe-B ribbons at room temperature.

Composition	Lattice constant a (Å)	Lattice constant c (Å)	H_c (kOe)	$(BH)_{max}$ (MGOe)	T_c (ºC)
$MM_{12}Fe_{82}B_6$	8.79	12.22	4.93	10.85	249
$MM_{11}Nd_1Fe_{82}B_6$	8.80	12.24	5.38	12.20	
$MM_{10}Nd_2Fe_{82}B_6$	8.80	12.23	5.95	13.77	
$MM_8Nd_4Fe_{82}B_6$	8.80	12.23	7.81	15.41	291
$MM_5Nd_7Fe_{82}B_6$	8.81	12.22	8.54	16.96	
$MM_2Nd_{10}Fe_{82}B_6$	8.81	12.22	10.71	18.64	337
$Nd_{12}Fe_{82}B_6$	8.81	12.22	10.94	21.07	346

The intergranular exchange coupling effect is dependent on the microstructure, which could be investigated by Henkel plots via the formula, $\delta m = [2M_r(H) + M_d(H)]/M_r - 1$ [24]. Here $M_r(H)$ is the initial remanence obtained by the application and then the subsequence removal of applied field H on the thermal demagnetized sample, $M_d(H)$ is the demagnetization remanence obtained in opposite direction for the sample magnetized to saturation in positive direction, and M_r is the remanence for the sample magnetized to saturation. Fig. 4 shows the δm curves for all the samples at room temperature. The positive value of δm implies the dominant exchange coupling effect over the dipolar interaction. With the increase of Nd content the maximum of δm value increases. In $MM_{12}Fe_{82}B_6$ and $MM_{11}Nd_1Fe_{82}B_6$ the contents of La-Ce are less than that in $Nd_2Ce_{10}Fe_{82}B_6$, but the maximum of δm value is much lower in $MM_{12}Fe_{82}B_6$ and $MM_{11}Nd_1Fe_{82}B_6$ [10]. The coexisting of more amounts of amorphous phase and minor phases would weaken the effect of intergranular exchange coupling and decrease the maximum of δm value [25]. So the appropriate addition of Nd is necessary to improve the crystallinity for decreasing the amount of amorphous phase and minor phases in these mischmetal-based ribbons. The maximum of δm value increases with Nd addition, indicating the enhancement of exchange

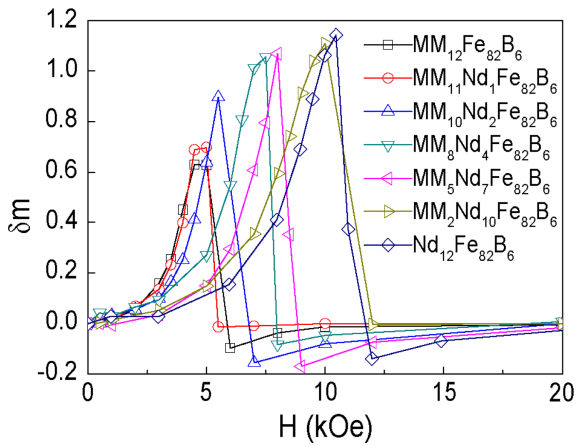

Fig. 4. (Color online) δm curves for (MM,Nd)-Fe-B ribbons at room temperature.

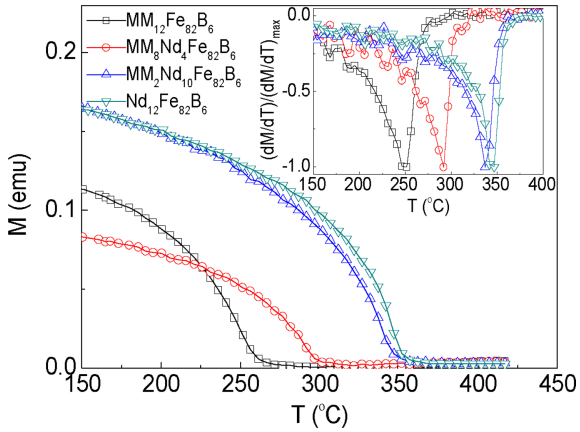

Fig. 5. (Color online) Magnetization versus temperature under the applied field of 1 kOe for (MM,Nd)-Fe-B ribbons.

coupling, and so the squareness of demagnetization curve improves.

It can further investigate the structure and magnetic properties via the temperature dependence of magnetization. As shown in Fig. 5, magnetized the sample to saturation firstly, and then increased the temperature and recorded the magnetization under the applied field of 1 kOe. The abrupt decrease of magnetization corresponds to the phase transition from the ferromagnetic to paramagnetic state at Curie temperature, at which the exchange energy is overcome by thermal fluctuation. With the decrease of mischmetal content, the phase transition temperature, i.e., Curie temperature increases. The inset of Fig. 5 shows the reduced value of *dM*/*dT*. It can be seen that with the increase of Nd content the half height width of *dM*/*dT* peak decreases, suggesting that the temperature span becomes narrowed in the magnetic phase transition. The structural disorder results in a larger temperature span in the magnetic phase transition [26]. For mischmetal-based magnets, the low crystallinity and the amorphous structure would lead to the non-uniform of the atomic distance, and the temperature span is broadened in the magnetic phase transition. For Nd substitution for mischmetal the decrease of the temperature span in magnetic phase transition also indicates that the appropriate addition of Nd could improve the crystallinity of $R_2Fe_{14}B$ crystal phase, which is necessary to enhance the coercivity in the mischmetal-based magnets.

4. Conclusions

In summary, mischmetal-based magnets were prepared and the magnetic properties were investigated in $MM_{12-x}Nd_xFe_{82}B_6$ (0~12) ribbons. The crystallinity of $R_2Fe_{14}B$ phase is a little weaker in $MM_{12}Fe_{82}B_6$ ribbons, and it is improved with Nd substitution for mischmetal. The lattice constants of $(MM,Nd)_2Fe_{14}B$ increase slightly for a little amount of Nd substitution but decreases for a large amount substitution. Both the coercivity and the squareness of hysteresis loop improve with the increase in the Nd substitution amount. The increase of squareness should be partially attributed to the improvement in the crystallinity of $R_2Fe_{14}B$ crystal phase. In $MM_5Nd_7Fe_{82}B_6$ ribbons the content of La-Ce is nearly the same with Ce content in $Ce_4Nd_8Fe_{82}B_6$, and the coercivities are nearly the same, indicating that it is reasonable to prepare the resource-saving rare-earth magnets using the less costly mischmetal. Optimizing the composition designing for improving the crystallinity of $R_2Fe_{14}B$ crystal phase is necessary to enhance the magnetic properties in the mischmetal-based permanent magnets.

Acknowledgements

The present work was supported by the National Natural Science Foundation of China (No. 51861030), and the National Key Research and Development Program of China (No. 2016YFB0700900).

References

[1] S. X. Zhou, Y. G. Wang, and R. Høier, J. Appl. Phys. **75**, 6268 (1994).
[2] M. G. Zhu, W. Li, J. D. Wang, L. Y. Zheng, Y. F. Li, K. Zhang, H. B. Feng, and T. Liu, IEEE Trans. Magn. **50**, 1000104 (2014).
[3] A. K. Pathak, M. Khan, K. A. Gschneidner Jr, R. W. McCallum, L. Zhou, K. Sun, M. J. Kramer, and V. K. Pecharsky, Acta Mater. **103**, 211 (2016).
[4] T. Y. Ma, B. Wu, Y. J. Zhang, J. Y. Jin, K. Y. Wu, S. Tao, W. X. Xia, and M. Yan, J. Alloys Compd. **721**, 1 (2017).
[5] M. Hussain, L. Z. Zhao, C. Zhang, D. L. Jiao, X. C. Zhong, and Z. W. Liu, Physica B **483**, 69 (2016).
[6] Z. Li, W. Liu, S. Zha, Y. Li, Y. Wang, D. Zhang, M. Yue, J. Zhang, and X. Huang, J. Magn. Magn. Mater. **393**, 551 (2015).
[7] Q. R. Yao, Y. H. Shen, P. C. Yang, H. Y. Zhou, G. H. Rao, J. Q. Deng, Z. M. Wang, and Y. Zhong, J. Rare Earth. **34**, 1121 (2016).
[8] X. D. Fan, K. Chen, S. Guo, R. J. Chen, D. Lee, A. Yan, and C. Y. You, Appl. Phys. Lett. **110**, 172405 (2017).
[9] B. J. Ni, H. Xu, X. H. Tan, and X. L. Hou, J. Magn. Magn. Mater. **401**, 784 (2016).
[10] Z. B. Li, B. G. Shen, M. Zhang, F. X. Hu, and J. R. Sun, J. Alloys Compd. **628**, 325 (2015).
[11] K. Pei, X. Zhang, M. Lin, and A. Yan, J. Magn. Magn. Mater. **398**, 96 (2016).
[12] B. Peng, T. Ma, Y. Zhang, J. Jin, and M. Yan, Scr. Mater.

131, 11 (2017).
[13] K. Y. Ko, S. Yoon, and J. G. Booth, J. Magn. Magn. Mater. **176**, 313 (1997).
[14] Z. R. Zhao, X. Wang, X. F. Zhang, Q. Ma, Y. L. Liu, Y. F. Li, F. Liu, and G. F. Wang, J. Magn. **22**, 60 (2017).
[15] X. Q. Yu, M. Yue, W. Q. Liu, Z. Li, M. G. Zhu, and S. Z. Dong, J. Rare Earth. **34**, 614 (2016).
[16] J. F. Herbst, Rev. Mod. Phys. **63**, 819 (1991).
[17] A. Alam, M. Khan, R. W. McCallum, and D. D. Johnson, Appl. Phys. Lett. **2**, 042402 (2013).
[18] J. Jin, Y. Zhang, G. Bai, Z. Qian, C. Wu, T. Ma, B. Shen, and M. Yan, Sci. Rep. **6**, 30194 (2016).
[19] J. F. Herbst, M. S. Meyer, and F. E. Pinkerton, J. Appl. Phys. **111**, 07A718 (2012).
[20] C. J. Yan, S. Guo, R. J. Chen, D. Lee, and A. R. Yan, Chin. Phys. B **23**, 107501 (2014).
[21] G. C. Hadjipanayis, Y. F. Tao, and K. Gudimetta, Appl. Phys. Lett. **47**, 757 (1985).
[22] T. W. Capehart, R. K. Mishra, G. P. Meisner, C. D. Fuerst, and J. F. Herbst, Appl. Phys. Lett. **63**, 3642 (1993).
[23] D. P. Kozlenko, K. Drużbicki, S. E. Kichanov, E. V. Lukin, H. P. Liermann, K. V. Glazyrin, and B. N. Savenko, Phys. Rev. B **95**, 054115 (2017).
[24] P. E. Kelly, K. O'Grady, P. I. Mayo, and R. W. Chantrell, IEEE Trans. Magn. **25**, 3881 (1989).
[25] Z. B. Li, M. Zhang, L. C. Wang, B. G. Shen, X. F. Zhang, Y. F. Li, F. X. Hu, and J. R. Sun, Appl. Phys. Lett. **104**, 052406 (2014).
[26] C. Mayer, S. Gorsse, G. Ballon, R. Caballero-Flores, V. Franco, and B. Chevalier, J. Appl. Phys. **110**, 053920 (2011).